2009 International Symposium on Nonlinear Theory and its Applications
NOLTA'09, Sapporo, Japan, October 18-21, 2009

# Synthesis and analysis of a pulse-coupled spiking oscillator with simple structure

Tadashi Tsubone and Yasuhiro Wada

The Department of Electrical Engineering, Nagaoka University of Technology,
1603–1 Kamitomioka–cho, Nagaoka–shi, Niigata, 940–2188 Japan, tsubone@vos.nagaokaut.ac.jp

**Abstract**—In this paper, we propose a simple spiking oscillator which consists of 2-D linear sub-circuit, 1-D linear sub-circuit and instantaneous switchings. The spiking oscillator behaves chaotic motions and generates various spike trains. We provide the rigorous analysis of the nonlinear phenomena including hyperchaos generation. The dynamics of the system is governed by 2-D piecewise linear return map, therefore, the rigorous analysis can be performed. We provide the 2-D return map to consider parameter conditions for generation of various spike trains and the stability analysis of the observed phenomena.

## 1. Introduction

Synthesis and analysis of simple chaotic oscillators is a fundamental and interesting problem. The chaotic spiking oscillators (abbr. CSO) have been studied in several interesting works [1]-[3]. CSOs are closely related to resonant-and-fire neuron models [4]. CSOs are included in hybrid dynamical systems with various nonlinear phenomena and its coupled systems can be developed into efficient applications of neural networks [5]. The simple circuit implementation and the rigorous analysis of CSOs are important.

This paper consider a three dimensional CSO which consists of 2-D linear sub-circuit, 1-D linear sub-circuit and instantaneous switchings. The spiking oscillator behaves hyperchaotic motions and generates various spike trains. The basic concept for synthesis of the system is based on the previous works of 2-D and 1-D chaotic spiking oscillators in [6][7]. In these works, we provide that the dynamics of the CSOs is governed by 1-D piecewise linear return map. The piecewise linear map might enable us to perform the rigorous proof of chaos generation and and some remarkable analysis.

In this paper, we synthesize CSO whose dynamics is described by 2-D and 1-D linear equations connected to each other the instantaneous switching. Hence the system dynamics is formulated by 3-D linear equations with jump mechanism. And we show the system dynamics can be reduced to that of a 2-D return map that is non-invertible and is exactly piecewise linear. The 2-D return map can be described explicitly. Using the return map, we give a theoretical evidence for hyperchaos generation, where we define the hyperchaos as an attractor whose 2-D return map is stretching in almost all directions. First, we introduce a 2-D spiking oscillator[7] as the basic chaotic system. Second, an 1-D spiking oscillator[6] is also shown, and finally we propose the coupled spiking oscillator with 3-D dynamics.

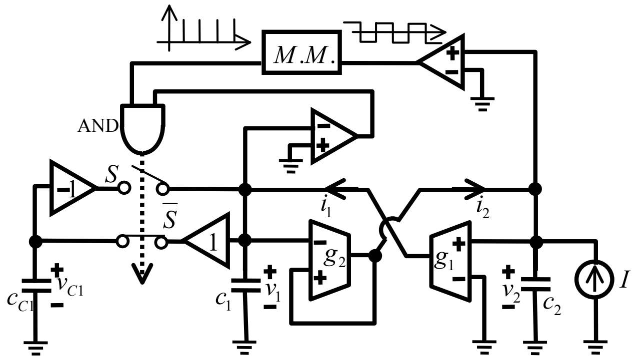


Figure 1: 2-D chaotic spiking oscillator.

## 2. Two dimensional spiking oscillator

### 2.1. Circuit and dynamics

Figure 1 shows the circuit model of the 2-D chaotic spiking oscillator. When $S$ is opened, the circuit dynamics is described by

$$\begin{pmatrix} C_1 \dfrac{dv_1}{dt} \\ C_2 \dfrac{dv_2}{dt} \end{pmatrix} = \begin{pmatrix} 0 & g_1 \\ -g_2 & g_2 \end{pmatrix} \begin{pmatrix} v_1 \\ v_2 \end{pmatrix} + \begin{pmatrix} 0 \\ I \end{pmatrix}, \qquad (1)$$

where $I$ is a constant current. Using the following dimensionless variables and parameters

$$\tau = \sqrt{\frac{g_1 g_2}{C_1 C_2}}t, \quad x = \frac{g_2}{I}v_1, \\ y = \frac{g_2}{I}\sqrt{\frac{C_2 g_1}{C_1 g_2}}v_2, 2\delta = \sqrt{\frac{C_1 g_2}{C_2 g_1}}, \qquad (2)$$

Equation (1) is transformed into

$$\begin{cases} \dot{x} = y, \\ \dot{y} = 2\delta y - x + 1, \end{cases} \qquad (3)$$

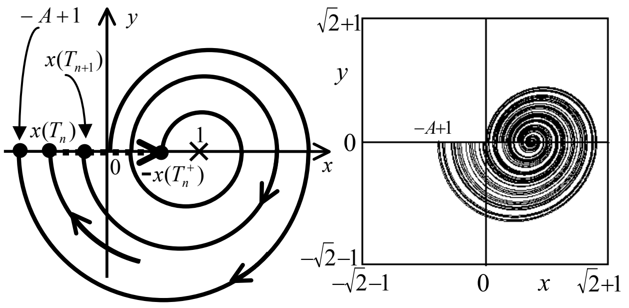


Figure 2: Behavior of Trajectories on the phase space and a typical chaos attractor. ($\delta \simeq 0.11$)

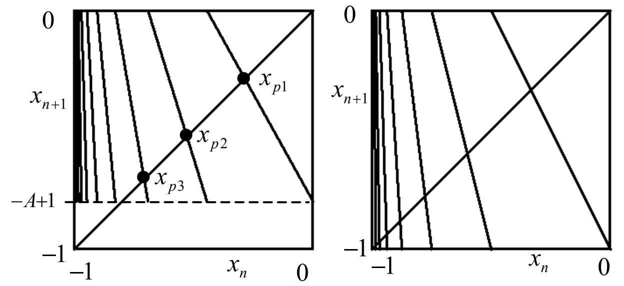


Figure 3: Chaotic return maps. (left: $A = 1.8(\delta \simeq 0.09)$, right: $A \to 2(\delta \simeq 0.11)$).

where "·" represents the derivative of $\tau$. Here, we assume the following parameter condition:

$$0 < \delta < 1. \tag{4}$$

In this parameter range, Equation (3) has unstable complex characteristic roots $\delta \pm j\omega$, where $\omega = \sqrt{1-\delta^2}$. The trajectory on the phase space moves around the equilibrium point $(1, 0)$ divergently and it must reach to the fourth quadrant on the half line $l_{Th} = \{(x, y)|x < 0, y = 0\}$ as shown in the left figure of Fig. 2.

In this circuit in Fig. 1, *M.M.* is a monostable multivibrator which outputs pulse signals to close the switch $S$ and to open $\bar{S}$ instantaneously. Two comparators detect the impulsive switching condition. If $v_1 \geq 0$ or $v_2 \leq 0$, the switch $S$ is opened and $\bar{S}$ is closed. For the meantime, the voltage $v_1$ is stored in $C_{C1}$. If $v_1 < 0$ and $v_2 > 0$, then *M.M.* is triggered by the pair of comparators, and the switch $S$ is closed and $\bar{S}$ is opened instantaneously. At that time, the voltage $v_1$ is reset to the inverse voltage $-v_1$ instantaneously, by holding the continuity property of $v_2(t)$, that is,

$$\begin{aligned}[v_1(t^+), v_2(t^+)]^T &= [-v_1(t), v_2(t)]^T \\ &\text{for } v_1(t) < 0 \text{ and } v_2(t) > 0,\end{aligned} \tag{5}$$

where $t^+ \equiv \lim_{\varepsilon \to 0}\{t + \varepsilon\}$.

Because the parameter condition (4), the trajectory must reach $l_v \equiv \{(v_1, v_2)|v_1 < 0, v_2 = 0\}$ when the switchings occur. Namely, the normalized trajectory must hit $l_{Th}$, and jumps from $(x(T_n), 0)$ to $(-x(T_n^+), 0)$ as shown in the left figure of Fig. 2, where $T_n$ is the $n$-th switching moments.

Consequently, Eqn. (1) and (5) with the condition (4) are transformed into

$$\begin{aligned}&\left\{\begin{array}{l}\dot{x} = y, \\ \dot{y} = 2\delta y - x + 1,\end{array}\right. \text{ for } S = \text{off}, \\ &[x(\tau^+), y(\tau^+)]^T = [-x(\tau), 0]^T \\ &\qquad\qquad \text{for } x(\tau) < 0 \text{ and } y(\tau) = 0, \\ &(0 < \delta < 1).\end{aligned} \tag{6}$$

Now the system is characterized by only one parameter $\delta$. The right figure of Fig. 2 shows a typical chaotic attractor with $\delta \simeq 0.11$.

## 2.2. Analysis

The exact piecewise solution of Eqn. (18) for $S$ =off is derived as follows:

$$\begin{aligned}x(\tau) = e^{\delta\tau}\Big\{&\{x(0) - 1\}\cos\omega\tau \\ &+ \tfrac{1}{\omega}\{y(0) - \delta x(0) + \delta\}\sin\omega\tau\Big\} + 1.\end{aligned} \tag{7}$$

Here, let us focus on a trajectory starting from origin at $\tau = 0$ (see Fig. 2). The trajectory rotates divergently around the equilibrium point $(1, 0)$ and reaches the switching threshold at $\tau = \frac{2\pi}{\omega}$. A $x-$coordinate of the reaching point is obtained as $-e^{\frac{2\pi\delta}{\omega}} + 1$, by substituting $x(0) = 0$ and $\tau = \frac{2\pi}{\omega}$ into (7). Here we define $A \equiv e^{\frac{2\pi\delta}{\omega}} > 1$ and $l \equiv \{(x, y)| - 1 < x < 0, y = 0\}$. And we consider the case of $-A + 1 > -1$, In this case, the trajectory starting from $l$ must jump instantaneously to the symmetric point of the origin, the trajectory rotates $k-$times ($k = 1, 2, 3, \cdots$) around the equilibrium point and it must return to $l$ after $\frac{2k\pi}{\omega}$. We henceforth consider the following parameter range with (4):

$$1 < A < 2. \tag{8}$$

If we choose $l$ as Poincaré-section, we can define one dimensional return map $f$ from $l$ to itself. Letting $(x(T_n), 0)$ be the starting point, $(x(T_{n+1}), 0)$ be the return point as shown in left figure of Fig. 2. And letting any points on $l$ be represented by its $x$-coordinate, $f$ is defined by

$$f : l \mapsto l, \quad x_{n+1} = f(x_n), \tag{9}$$

where we rewrite $x_n = x(T_n)$.

Substituting $x(0) = -x_n$ and $\tau = \frac{2k\pi}{\omega}$ into the solution (7), we obtain an explicit expression for the function $f$:

$$f(x_n) = \left\{\begin{array}{l} -A(x_n + 1) + 1 \\ \qquad \text{for } \frac{1}{A} - 1 < x_n \leq 0, \\ \qquad\qquad \vdots \\ -A^k(x_n + 1) + 1 \\ \qquad \text{for } \frac{1}{A^k} - 1 < x_n \leq \frac{1}{A^{k-1}} - 1, \\ \qquad\qquad \vdots \\ \qquad\qquad (k = 1, 2, 3, \cdots),\end{array}\right. \tag{10}$$

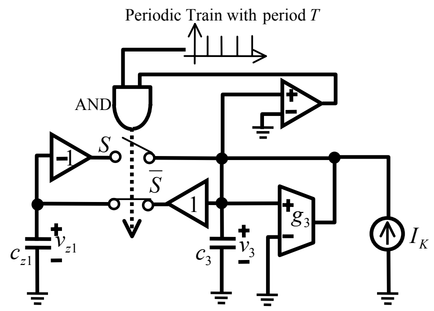


Figure 4: 1-D chaotic spiking oscillator.

where each border of the piecewise maps, $Th_k = \frac{1}{A^k} - 1$, are derived by solving $0 = -A^k(Th_k + 1) + 1$. Typical return map $f$ are shown in Fig. 4. In this figure, $k$-th branch from the right corresponds to a trajectory with a $k$ turn spiral on the phase space.

Here, we give the proof for chaos generation of this system. From condition (8), $|\frac{\partial f}{\partial x_n}| > 1$ is satisfied without discontinuous points and $f(l) \subset l$ is obvious, hence $f$ exhibits chaos.

## 3. One dimensional spiking oscillator

Figure 4 shows the circuit model of the 1-D chaotic spiking oscillator. In a similar way to Sec. 2, We can describe the circuit dynamics when $S$ is opened.

$$C_3 \frac{dv_3}{dt} = g_3 v_3 + I_k. \tag{11}$$

where $I_k$ is a constant current. Using the following dimensionless variables and parameters

$$\tau = \frac{1}{T} t, \quad z = \frac{g_3}{I_k} v_3, \quad \lambda = \frac{g_3 T}{C_3}, \tag{12}$$

Equation (11) is transformed into

$$\dot{z} = \lambda(z + 1). \tag{13}$$

Here, we assume the following parameter condition:

$$0 < \lambda < \ln 2. \tag{14}$$

The switching mechanism is similar to 2-D system. Where the switching operation depend on the external pulse train with period $T$. When $S$ is closed, the voltage $v_3$ is reset to the inverse voltage $-v_3$ instantaneously.

$$v_3(t^+) = -v_3(t) \qquad \text{for } v_3(t) > 0 \text{ and } t = kT \quad (k = 1, 2, 3, \cdots), \tag{15}$$

Because the parameter condition (14), If the initial condition is set as $-1 < z(0) < 0$, z(1) must exists on $(-1, 1)$.

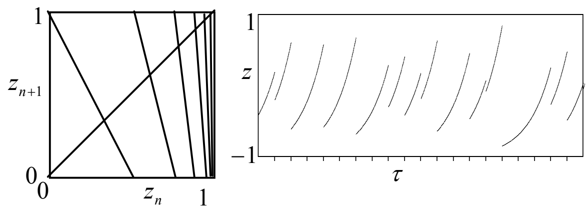


Figure 5: Chaotic return maps and time domain waveform. ( $a \to 2(\lambda \simeq 0.69)$).

Consequently, Eqn. (11) and (15) with the condition (**??**) are transformed into

$$\begin{aligned} &\dot{z} = \lambda(z + 1), && \text{for } S = \text{off}, \\ &z(\tau^+) = -z(\tau) && \text{for } z(\tau) > 0 \text{ and } \tau = k, \\ &(0 < \lambda < \ln 2). \end{aligned} \tag{16}$$

Here, we can define one dimensional return map $g$ in the similar way to Sec. 2. Let $z_n$ be the state at the $n$-th switching moment. Then the relationship $z_{n+1} = g(z_n)$ can be obtained as the following an explicit expression:

$$g(z_n) = \begin{cases} B(-z_n + 1) - 1 \\ \quad \text{for } 0 < z_k \leq 1 - \frac{1}{B}, \\ \quad \vdots \\ B^k(-z_n + 1) + 1 \\ \quad \text{for } 1 - \frac{1}{B^{k-1}} < z_n \leq 1 - \frac{1}{B^k}, \\ \quad \vdots \\ \quad (k = 1, 2, 3, \cdots), \end{cases} \tag{17}$$

where $B = e^{\lambda}$. Typical return map $g$ and the corresponding are time-domain waveform are shown in Fig. 5. In this figure,

The proof for chaos generation of this system can be given irrefutable, because $|\frac{\partial g}{\partial z_n}| > 1$ is satisfied without discontinuous points and $g(l_0) \subset l_0$ ($l_0 = \{0, 1\}$) is obvious in the condition (14).

## 4. A pulse-coupled spiking oscillator

Figure 6 shows the circuit model of the 3-D chaotic spiking oscillator. The normalized dynamics can be represented as the followings in a similar way to Sec. 2 and 3.

$$\begin{aligned} &\begin{cases} \dot{x} = y, \\ \dot{y} = 2\delta y - x + 1, & \text{for } S = \text{off}, \\ \dot{z} = \lambda z + K, \end{cases} \\ &[x(\tau^+), y(\tau^+), z(\tau^+)]^T = [-x(\tau), 0, -z(\tau)]^T \\ &\qquad \text{for } x(\tau) < z(\tau) \text{ and } y(\tau) = 0, \\ &(0 < \delta < 1). \end{aligned} \tag{18}$$

Now the system is characterized by three parameter $\delta$, $\lambda$ and $K$. The Fig. 7 shows a typical chaotic attractor and time-domain waveform. Also, the return map can be de-

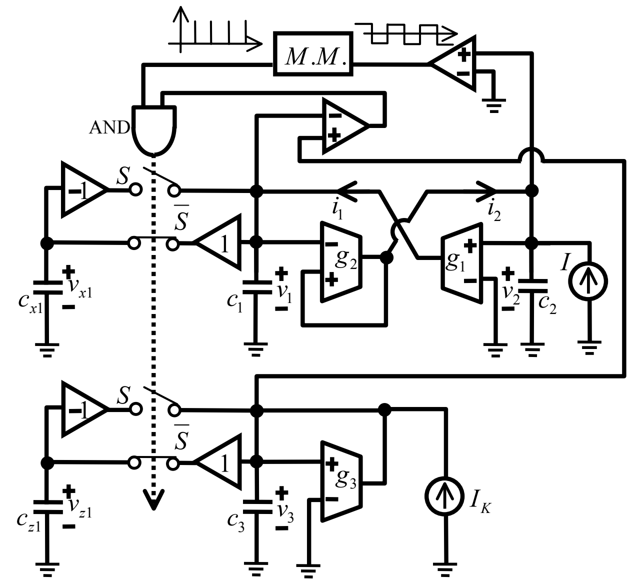


Figure 6: 3-D chaotic spiking oscillator.

rived explicitly. Let $[x_n, z_n]^T$ be the state at the $n$-th switching moment. Then the two dimensional return map form $[x_n, z_n]^T$ to $[x_{n+}, z_{n+}]^T$ can be obtained as the followings

$$\begin{bmatrix} x_{n+1} \\ z_{n+1} \end{bmatrix} = \begin{cases} \begin{bmatrix} (-a)(-x_n-1)+1 \\ b(-z_n+c)-c \end{bmatrix} \text{ for } \begin{bmatrix} x_n \\ z_n \end{bmatrix} \in S_1 \\ \vdots \\ \begin{bmatrix} (-a)^k(-x_n-1)+1 \\ b^k(-z_n+c)-c \end{bmatrix} \text{ for } \begin{bmatrix} x_n \\ z_n \end{bmatrix} \in S_k \\ \vdots \\ (k = 1, 2, 3, \cdots), \end{cases} \tag{19}$$

$$\begin{aligned} S_0 &= \{(x,z)|z > x\}, \\ S_1 &= S_0 \cap \{(x,z)|z < \tfrac{1}{b}\{(-a)(x+1)-(c+1)\}+1\} \\ S_2 &= S_0 \cap \overline{S_1} \\ &\quad \cap\{(x,z)|z < \tfrac{1}{b^2}\{(-a)^2(x+1)-(c+1)\}+1\} \\ &\quad \vdots \\ S_k &= S_0 \cap \overline{S_1} \cap \overline{S_2} \cap \cdots \cap \overline{S_{k-1}} \\ &\quad \cap\{(x,z)|z < \tfrac{1}{b^k}\{(-a)^k(x+1)-(c+1)\}+1\} \\ &\quad \vdots \end{aligned}$$

weber $a = e^{\frac{\delta\pi}{\omega}}$, $b = e^{\frac{\lambda\pi}{\omega}}$ and $c = \frac{K}{\lambda}$. We can give the proof for hyperchaos generation from this return map. $|\frac{\partial x_{n+1}}{\partial x_n}| > 1$ and $|\frac{\partial z_{n+1}}{\partial z_n}| > 1$ are guaranteed : the return map is stretching almost everywhere on $S_0$. Therefore in order to prove hyperchaos generation, it is sufficient that the map has an attractor on $S_0$. The sufficient condition have been reported in [8].

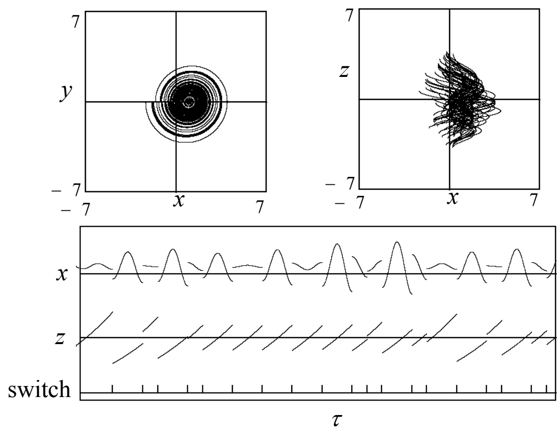


Figure 7: Chaotic return maps and time domain waveform. ( $\delta = 0.05, \lambda = 0.05, K = 0.5$).

## 5. Conclusion

This paper considered a simple spiking oscillator which consists of 2-D linear sub-circuit, 1-D linear sub-circuit and instantaneous switchings. The spiking oscillator behaves hyperchaotic motions and generates various spike trains. The dynamics of the system is governed by 2-D piecewise linear return map, therefore, the rigorous analysis can be performed. Some analytical results by using the 2-D return map will provided in the near future.

## References


[1] K.Mitsubori and T.Saito, "Dependent switched capacitor chaos generator and its synchronization, "IEEE Trans. Circuit Syst. I, 44, 12, pp.1122-1128 (1997).

[2] H. Nakano and T. Saito, "Grouping synchronization in a pulse-coupled network of chaotic spiking oscillators, "IEEE Trans. Neural Networks, 15, 5, pp. 1018-1026 (2004).

[3] Y. Takahashi, H. Nakano and T.Saito, "A simple hyperchaos generator based on impulsive switching," IEEE Trans. CAS-II, vol. 51, no. 9, pp. 468-472, (1998).

[4] Izhikevich, "Dynamical systems in neuroscience, " MIT Press, (2006).

[5] H. Nakano and T. Saito, "Basic dynamics from an integrate-and-fire chaotic circuits with a periodic input," IEICE Trans. Fundamentals, Vol. E84-A, No. 5, pp.1293-1300 (2001).

[6] Tadashi Tsubone and Noriyoshi Kambayashi, "Chaos and Periodic Oscillation of a Multirate Sampled-Data Dynamical System,"IEICE Trans. Fundamentals., Vol. E90-A, No. 9, pp. 1924-1931, (2007).

[7] Tadashi Tsubone and Yasuhiro Wada, "Stabilizing Unknown Periodic Orbits of a Chaotic Spiking Oscillator," IEICE Trans. Fundamentals., Vol. E92-A, No. 5, pp. 1308-1315, (2009).

[8] Tadashi Tsubone and Toshimichi Saito, "Hyperchaos from 4-D Manifold Piecewise-Linear System," IEEE Trans. CAS-I, vol. 45, no. 9, pp. 889-894, (1998)